

The Expression and Regulation of the Nuclear Receptor-Binding SET Domain Protein 2 in Parotid Carcinoma

Gu M¹, Ge J¹, Pan Q¹, Wang P¹ and Hua F^{2*}

¹Department of Stomatology, The Third Affiliated Hospital of Soochow University, The First People's Hospital of Changzhou, Changzhou City, Jiangsu Province, China, 213003

²Department of Endocrinology, The Third Affiliated Hospital of Soochow University, The First People's Hospital of Changzhou, Changzhou City, Jiangsu Province, China, 213003

*Corresponding author:

Fei Hua,
Department of Endocrinology, The Third Affiliated Hospital of Soochow University, The First People's Hospital of Changzhou, Changzhou City, Jiangsu Province, 213003, China

Received: 02 Sep 2023

Accepted: 16 Oct 2023

Published: 24 Oct 2023

J Short Name: AJSCCR

Copyright:

©2023 Hua F, This is an open access article distributed under the terms of the Creative Commons Attribution License, which permits unrestricted use, distribution, and build upon your work non-commercially.

Citation:

Hua F. The Expression and Regulation of the Nuclear Receptor-Binding SET Domain Protein 2 in Parotid Carcinoma. *Ame J Surg Clin Case Rep.* 2023; 7(1): 1-6

Keywords:

Parotid carcinoma; NSD-2; proliferation; Invasion; Apoptosis

Abbreviation:

NSD: Nuclear Receptor-Binding SET Domain; WHS: Wolf-Hirschhorn Syndrome; WHSC1: Wolf-Hirschhorn Syndrome Candidate 1; NEK7: NI-MA-Related-Kinase-7; PBS: Phosphate Buffered Saline; CCK8: Cell Counting Kit-8

1. Abstract

1.1. Background: To explore the effect of down-regulating NSD2 gene expression on proliferation, apoptosis and invasion of parotid carcinoma.

1.2. Materials and Methods: SACC-2 cells were transfected with NSD2 siRNA. Real-time quantitative PCR was used to detect expression of NSD2 mRNA and western blot was used to detect the expression of NSD2 protein. CCK-8 and colony formation test were used to detect cell proliferation. Annexin V PI double staining flow cytometry was used to detect apoptosis, cell scratch and trans-well test were used to detect cell invasion.

1.3. Results: The apoptosis rates of siNSD2-1 and siNSD2-2 groups were significantly higher. The wounds of siNSD2-1 and siNSD2-2 group were more significant than that of control, and relative migration distances were reduced significantly than that of control ($P < 0.05$). The cells which penetrated cell membrane of siNSD2-1 and siNSD2-2 were significantly less than those of control ($P < 0.05$).

1.4. Conclusions: Silencing NSD2 gene can inhibit the proliferation and invasion of parotid carcinoma SACC-2 cells and induce apoptosis.

2. Introduction

Neoplasms of the parotid gland remain rare cancers and, although their incidence has increased in recent decades, relatively few risk

factors have been identified [1]. The etiology of parotid carcinoma remains vague. Epigenetics is the study of heritable phenotype changes that do not involve alterations in the DNA sequence [2]. Epigenetic alterations of DNA repair genes or cell cycle control genes are very frequent in sporadic (non-germ line) cancers [3], including parotid carcinoma. Epigenetic modifiers are widely recognized as targets for anti-cancer therapeutic intervention, due to their critical roles in regulating gene expression and chromatin integrity in addition to their dysregulation in multiple human cancers. In particular, the NSD (nuclear receptor-binding SET domain) family of histone lysine methyltransferase enzymes, NSD1, NSD2/WHSC1/MMSET, and NSD3/WHSC1L1, have all been implicated as cancer therapeutic targets [4].

Among the three members, NSD2 has been implicated as a therapeutic target for a variety of cancers. Because the gene is located within the Wolf-Hirschhorn syndrome (WHS) critical region of chromosome 4, NSD2 is also known as Wolf-Hirschhorn syndrome candidate 1 (WHSC1). [5] NSD2 is estimated 6% genetic and expression alteration rate in the head and neck cancer TCGA database. While most of these alterations are deletions or missense mutations, Saloura et al. found that NSD2 is moderately or strongly overexpressed in 73% of patients bearing head and neck cancer with locoregionally advanced disease and that this overexpression was significantly higher compared to normal squamous epithelium [6]. The levels of NSD2 increased significantly with the transi-

tion from normal squamous to dysplastic epithelium and then to head and neck cancer, supporting its pathogenetic role in the initial stages of head and neck cancer oncogenesis. A significant association of higher NSD2 expression with poor grade was found as well. Knockdown of NSD2 led to significant decrease in the cell viability of four head and neck cancer cell lines and to decreased levels of H3K36 dimethylation and trimethylation, indicating its non-redundant role in establishing H3K36 methylation levels in head and neck cancer. Furthermore, NSD2 directly regulated the transcription of NIMA-related-kinase-7 (NEK7), a cell cycle regulator necessary for progression into cytokinesis and mitotic spindle formation, and, accordingly, its knockdown delayed the cell-cycle progression of head and neck cancer cells. High expression of NSD2 protein has been demonstrated in many different human cancer types, including bladder, brain, gastrointestinal, lung, liver, ovary, skin and uterus [6-13]. But NSD2 has not been researched in parotid carcinoma yet.

In the present study, we aimed to examine the expression of NSD2 in parotid tissue and furthermore investigated the regulation mechanism of NSD2. To our best knowledge, there has been no other research focusing the important role of NSD2 in the development and progression of parotid carcinoma.

3. Methods and Materials

3.1. Patients

A total of 59 formalin-fixed paraffin-embedded parotid carcinoma tissues from 2010 to 2015 were obtained from Department of Otorhinolaryngology of our institute. Besides, 15 cases of pleomorphic adenoma were also collected as control. Written patient consent was obtained and the study was approved by the Ethics Committee of our institute. All the samples had been rechecked for the confirmed pathological diagnosis by pathologists.

3.2. Immunohistochemistry

The paraffin-embedded SACC tissues were cut into 4mm-thick sections, dewaxed in xylene, rehydrated and graded in ethanol solutions. Antigen was retrieved by heating the tissue sections at 100°C for 30 min in EDTA (1 mmol/L, pH = 9.0) solution, and the sections were later immersed in a 0.3% hydrogen peroxide solution for 30 min to block endogenous peroxidase activity. After rinsing with phosphate buffered saline (PBS) for 5 min, the tissue section was blocked with 3% BSA at room temperature for 30 min, and then incubated with rabbit anti-human NSD2 antibody (1: 200 dilution) at 4 °C overnight. Then, the tissue section was incubated with HRP-labeled goat anti mouse secondary antibody, followed by incubation with diaminobenzene as the chromogen, and hematoxylin as the nuclear counterstain. After that, the sections were dehydrated, cleared and mounted and further photographed under a microscope.

Two pathologists with no knowledge of the patients' information examined the stained sections independently. At high magnifica-

tion, 10 representative views are selected. Then strained tumor cells were counted. Extremely strong positive, strong positive, positive and negative were considered when the number of strained tumor cells were no less than 75%, no less than 50%, no less than 10% and less than 10%, respectively. Results from the two pathologists were averaged and used for statistical analysis.

3.3. Cell Culture

Human salivary adenoid cystic carcinoma cell lines SACC-2 were obtained from Chinese Academy of Sciences, Shanghai Institutes for Biological Sciences. The cells were cultured in DMEM supplemented with 10% FBS and incubated at standard culture conditions (5% CO₂, 37°C).

3.4. siRNA Transfection in SACC-2 Cells

For transfection, SACC-2 were seeded at each 1.5×10⁵ cells/well in a 6-well dish and were transfected with 100 ng/L siRNA against NSD2 using Lipofectamine RNAi-MAX (Life Technologies, Carlsbad, USA) in accordance with the manufacturer's instructions. NSD2 siRNA sequences were designed after selecting appropriate DNA targets as follows: NSD2: 5'-CATACATGAATGGGAAGCCTCTCTT-3'; NSD2 siRNA-2: 5'-CGACATAGGGAAGAGTACTCCTCAA-3'.

3.5. Western Blot Analysis

Proteins were prepared as described previously. Briefly, 1×10⁷ cells were homogenized briefly in 200µl of lysis buffer containing (in mM) 20 Tris-HCl (pH = 7.4), 150 NaCl, 2.5 EDTA, 50 NaF, 0.1 Na₄P₂O₇, 1 Na₃VO₄, 1 PMSF, 1 DTT, 0.02% (v/v) protease cocktail (Sigma-Aldrich, Missouri, USA), 1% (v/v) Triton X-100 and 10% (v/v) glycerol. The homogenates were centrifuged twice at 20,000 g at 4°C for 15 min, and the supernatants were saved as total proteins. Protein concentrations were determined by the BCA method. Equal amounts of proteins were separated by SDS-PAGE and transferred to a PVDF membrane (Bio-Rad, California, USA). Western blot analysis was performed under standard conditions with specific anti-NSD2 (Ab75359, Abcam, USA) antibody and anti-glyceraldehyde-3-phosphate dehydrogenase (GAPDH) (Ab8245, Abcam, USA). The immunoreaction was visualized using an enhanced chemiluminescent detection kit (Amersham, London, UK), exposed to X-ray film, and quantified by densitometry with a video documentation system (Gel Doc 2000, Bio-Rad, California, USA).

3.6. Cell Viability Assay

The cell viability was monitored using the Cell Counting Kit-8 (CCK8) (Dojindo Molecular Technologies, Kumamoto, Japan) according to the manufacturer's protocol. All of the experiments were repeated at least three times.

3.7. Colony Formation Assay

The cells were counted and seeded into six-well plates at a density of 500 cells per well and cultured for 14 d until the colonies were

visible. The cells were washed with phosphate-buffered saline (PBS) and fixed with paraformaldehyde for 15 min. The colonies were stained with Giemsa's solution for 15 min and washed with tap water. After air-drying, the colonies with more than 50 cells were counted.

3.8. Apoptosis Assay

Cells were centrifuged at 800 g at room temperature for 10 min and then collected and incubated in 24-well plate, with 1.0×10^5 cells in each well. Then NSD2 siRNA was transfected into cells and after 72h cells were collected. Cell apoptosis was detected according to the manufacturer's protocol of Annexin V/PI Detection Kit (Life Technologies, Carlsbad, USA) using flow cytometer (Thermo Fisher Scientific, Shanghai, China). All of the experiments were repeated at least three times.

3.10. Wound-healing assay

Cells were digested and seeded in 6-well culture plates with FBS deleted medium to inhibit cell proliferation. After being cultured to 80% confluence, the cells were scratched with a 200 ml pipette tip, washed with PBS, and replaced with FBS-free medium. Wounds were photographed under a microscope after scratching at 0 and 24 h, respectively.

3.11. Transwell for Cell Invasion Assay

The filters of Transwell chambers were coated with 30 mL of basement Matrigel at a dilution of 1:10 by serum-free medium. Cells were counted (25000) and resuspended in 200 mL serum-free medium, and then seeded in the upper chamber. The lower chamber received 600 mL of 10% FBS medium as a chemoattractant. After 24 h of incubation, cells above the filter were removed. The invaded cells at the bottom of filter were fixed in 4% paraformaldehyde and stained with 1% crystal violet. The cells were photographed and counted under an Olympus fluorescence microscope.

3.12. Statistical Analysis

All the statistical evaluations were analyzed by SPSS 13.0 software (SPSS Standard version 13.0, SPSS Inc.). All data were expressed as mean \pm standard error. Data were analyzed for statistical significance by using one-way ANOVA. $P < 0.05$ was considered statistically significant.

4. Results

4.1. Patient Characteristics

Amongst the 59 parotid carcinoma tissues, there were 24 cases of mucoepidermoid carcinoma, 12 cases of acinar cell carcinoma, 8 cases of lymphoepithelial carcinoma, 5 cases of adenoid cystic carcinoma and 10 cases of other types, respectively. Among them, 22 cases were male patients and the other 37 female, with an average of 52 y (20 – 86 y). None of the patients had received any anti-cancer therapy, no matter chemotherapy or radiotherapy or others. According to the UICC (1992) Staging criteria, there were 36 cases at stage I and stage II, and 23 at stage III and stage IV cases, respectively.

4.2. Expression of NSD2

Immunoreactivity for NSD2 protein was observed as brown, granular staining on the cell nuclei or in the plasma of tumor cells (Figure 1). The positive rates of NSD2 in parotid carcinoma and pleomorphic adenoma were 72.9% (43/59) and 40.0% (6/15), respectively ($P < 0.01$). In 36 cases at stage I and II, the NSD2 positive rate was 63.9% (23/36), and in 23 cases at stage III and IV, the NSD2 positive rate was 76.2% (20/23). However, the difference of NSD2 expression in subgroup III/IV and subgroup I/II was not statistical ($P = 0.0519$).

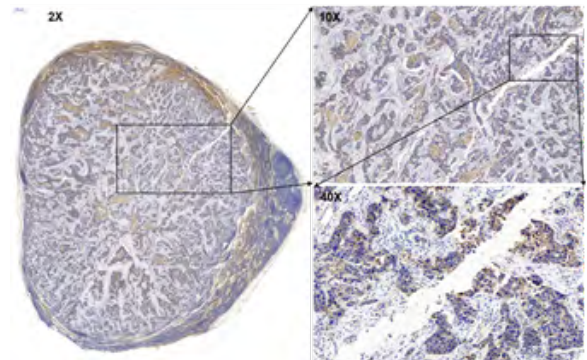


Figure 1: Positive NSD2 expression in adenoid cystic carcinoma ($\times 2$, $\times 10$, $\times 40$)

4.3. NSD2 siRNA Downregulates the Expression of NSD2 and Histone H3K36me2

Western blot results revealed that 72h after NSD2 siRNA was transfected into SACC-2 cells, the expression of NSD2 and histone H3K36me2 in SACC-2 cells decreased significantly comparing to control (Figure 2). For NSD2, the expression of siNSD2-1, siNSD2-2 and control were 0.238 ± 0.027 , 0.103 ± 0.017 and 1.129 ± 0.124 ($P < 0.05$). For H3K36me2, the expression of siNSD2-1, siNSD2-2 and control were 0.122 ± 0.018 , 0.09 ± 0.021 and 1.201 ± 0.108 , respectively ($P < 0.05$).

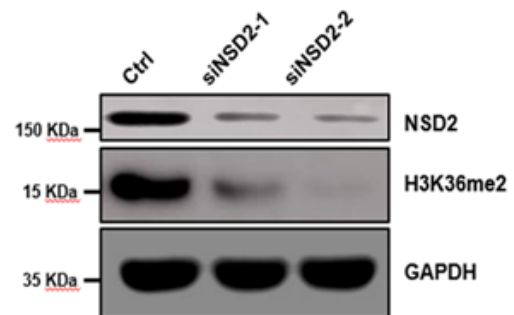


Figure 2: Seventy-two hours after NSD2 siRNA is transfected into SACC-2 cells, NSD2 and H3K36me2 are downregulated significantly

4.4. NSD2 siRNA Inhibits the Malignant Biological Ability of SACC-2 Cells

As results of CCK-8 assay, the growth curve was generated according to the A450 values in various time points (0h, 24h, 48h and 72h), by which the cell viability was calculated (Figure 3A). It was observed that siNSD2-1 and siNSD2-2 inhibited cell viability

of SACC-2 cells significantly, particularly in 72h ($P < 0.05$).

In colony formation assay, the number of formed colonies was calculated 14d after cultivated with soft agar. Colonies formed by cells transfected with siNSD2-1 and siNSD2-2 decreased significantly comparing to control ($P < 0.05$) (see Figure 3B). NSD2 siRNA could inhibit the ability of forming colony of SACC-2 cells.

Seventy-two hours after NSD2 siRNA was transfected into SACC-2 cells, the apoptosis rates of siNSD2-1 and siNSD2-2 groups were $(21.77 \pm 3.19) \%$ and $(29.84 \pm 2.78) \%$, while that of control was $(10.50 \pm 2.14) \%$ ($P < 0.05$). It is revealed that the inhibition of NSD2 expression can induce the apoptosis of SACC-2 cells (Figure 4).

Twenty-four hours after wound-healing cultivation, the wounds of siNSD2-1 and siNSD2-2 group were more significant than that of control, and the relative migration distances were reduced significantly than that of control as well ($P < 0.05$). It is concluded that the migration ability could be weakened via intervening the NSD2 expression in tumor cells (Figure 5).

Transwell assay revealed that the cells which penetrated cell membrane of siNSD2-1 (24.34 ± 3.58) and siNSD2-2 (24.34 ± 3.58) were significantly less than those of control (50.69 ± 9.57) ($P < 0.05$), suggesting that the invasion ability could be weakened via intervening the NSD2 expression in tumor cells (Figure 6).

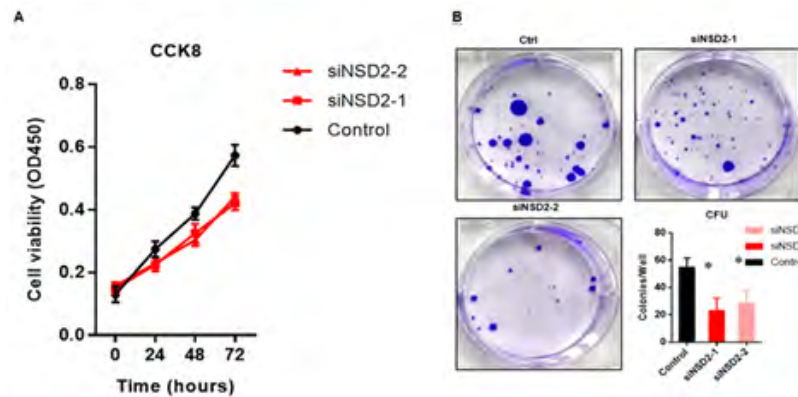


Figure 3: A. siNSD2-1 and siNSD2-2 inhibited cell viability of SACC-2 cells significantly, particularly in 72h ($P < 0.001$) B. Colonies formed by cells transfected with siNSD2-1 and siNSD2-2 decreased significantly comparing to control ($P < 0.05$)

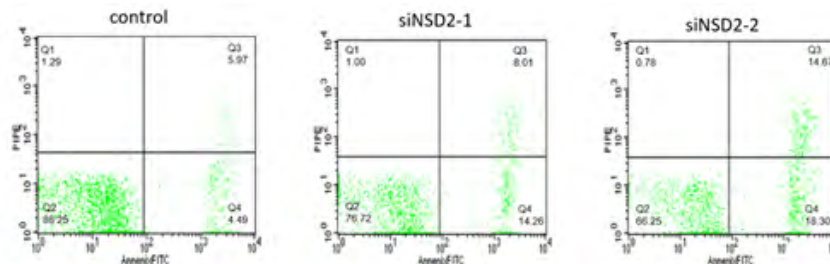


Figure 4: The apoptosis rates of siNSD2-1 and siNSD2-2 groups were $30.37 \pm 4.22\%$ and $35.17 \pm 3.43\%$, while that of control is $1.36 \pm 0.52\%$ ($P < 0.05$)

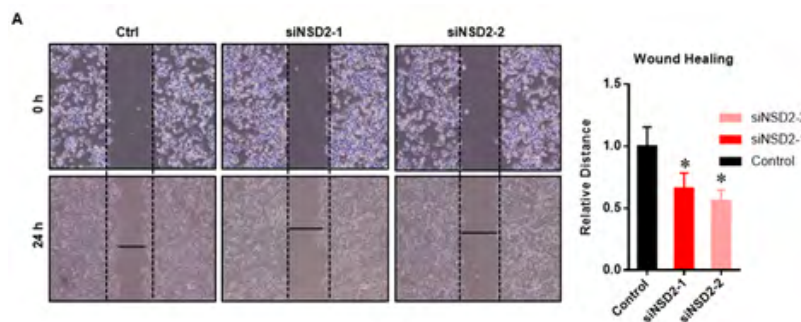


Figure 5: The wounds of siNSD2-1 and siNSD2-2 group are more significant than that of control, and the relative migration distances are reduced significantly than that of control as well ($P < 0.05$)

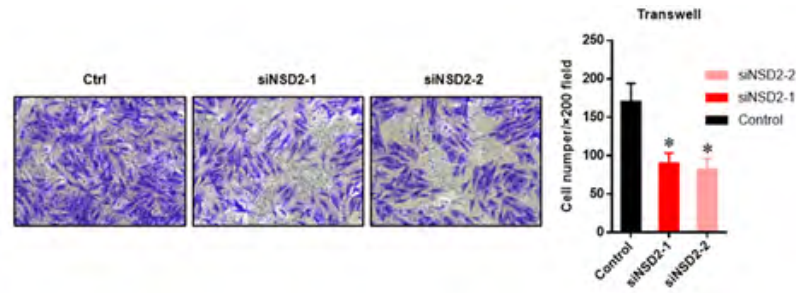


Figure 6: The cells which penetrate cell membrane of siNSD2-1 (24.34 ± 3.58) and siNSD2-2 (24.34 ± 3.58) were significantly less than those of control (50.69 ± 9.57) ($P < 0.05$)

5. Discussion

Management of parotid carcinoma, which consisting of various histological subtypes, is complex where therapeutic resistance contributes to significant morbidity. Therefore, prognostic biomarkers are urgently needed. In this study, we provide evidence that NSD2 is overexpressed in parotid carcinoma and that elevated NSD2 plays a major role in parotid carcinoma cell proliferation, migration, and invasion.

NSD2 has been reported to be upregulated in a number of solid cancers such as squamous cell carcinoma of the head and neck [6], endometrial cancer [9], lung cancer [7], neuroblastoma [10], bladder and colon cancer [10], hepatocellular carcinoma [14], ovarian carcinoma [11] and prostate cancer [15]. Overexpression in solid tumors appears to occur in the absence of genetic alterations. Additionally, NSD2 has been demonstrated to support the proliferation and/or survival of several cancer cell lines including myeloma cell lines with t (4;14) translocations [16, 17], leukemia cell lines carrying the E1099K mutation [18], prostate cancer [15, 19] and osteo and fibrosarcoma cell lines [17]. All these results are consistent with ours, that NSD2 promotes the malignant behaviors of various tumor cells.

The importance of NSD2 in above mentioned tumors has been previously demonstrated. However, its potential role in parotid carcinoma remains less understood. The present study is the first one which investigates the expression and function of NSD2 in parotid carcinoma.

It is worth noting that NSD2 expression has been reported to be detectable by immunohistochemistry in 77.8% of parotid carcinoma biopsies, significantly higher than in control. This makes NSD2 an attractive candidate for anti-parotid carcinoma therapy. Similar suggestion has been proposed for lung cancer.

The impact of the spreading of H3K36me2 into intergenic regions caused by cancer-context overexpressed NSD2 should not be underestimated since intergenic regions constitute a critical source of regulatory complexity in mammalian cells [20]. Top H3K36me2 regions contain important genes targeted by the RAS pathway. Additionally, regions chr12: 38161453-48300708 and chr8: 58830148-89198575 are both amplified and heavily marked with H3K36me2 in H1299 suggesting that the presence of this modifi-

cation reinforces the expression of amplified genes [21].

6. Conclusion

In conclusion, NSD2 gene might be associated with the invasion and metastasis of parotid carcinoma. Silence of NSD2 gene can inhibit the proliferation and invasion of parotid carcinoma cells, possibly via the regulation of H3K36me2 expression.

7. Conflicts of Interest

The undersigned authors warrant that the article is original, does not infringe on any copyright or other proprietary right of any third party, is not under consideration by another journal, and has not been previously published, whether in print or electronic media. There are no commercial or other associations that may pose a conflict of interest.

8. Funding Source

This study was funded by grants from Changzhou Sci&Tech Program (CJ20210092); Young Talent Development Plan of Changzhou Health Commission (CZQM2020025); Ideological and Political Program for Graduate Students of Soochow University (23124400); 2023 Soochow University Graduate Education Reform Achievement Award Cultivation Project (KY20231517) and Top Talent of Changzhou “14th Five-Year Plan” High-level Health Personnel Training Project (2022260).

References

1. Horn-Ross PL, Ljung BM, Morrow M. Environmental factors and the risk of salivary gland cancer. *Epidemiology*. 1997; 8: 414-9.
2. Dupont C, Arman DR, Brenner CA. Epigenetics: definition, mechanisms and clinical perspective. *Semin Reprod Med*. 2009; 27: 351-7.
3. Wood LD, Parsons DW, Jones S, Lin J, Sjoblom T. The genomic landscapes of human breast and colorectal cancers. *Science*. 2007; 318: 1108-13.
4. Bennett RL, Swaroop A, Troche C, Licht JD. The Role of Nuclear Receptor-Binding SET Domain Family Histone Lysine Methyltransferases in Cancer. *Cold Spring Harb Perspect Med*. 2017; 7.
5. Wiesmann UN, DiDonato S, Herschkowitz NN. Effect of chloroquine on cultured fibroblasts: release of lysosomal hydrolases and inhibition of their uptake. *Biochem Biophys Res Commun*. 1975; 66: 1338-43.
6. Saloura V, Cho HS, Kiyotani K, Alachkar H, Zuo Z. WHSC1 pro-

- motes oncogenesis through regulation of NIMA-related kinase-7 in squamous cell carcinoma of the head and neck. *Mol Cancer Res.* 2015; 13: 293-304.
7. Hudlebusch HR, Santoni-Rugiu E, Simon R, Ralfkiaer E, Rossing HH. The histone methyltransferase and putative oncoprotein MMSET is overexpressed in a large variety of human tumors. *Clin Cancer Res.* 2011; 17: 2919-33.
 8. Li J, Yin C, Okamoto H, Mushlin H, Balgley BM. Identification of a novel proliferation-related protein, WHSC1 4a, in human gliomas. *Neuro Oncol.* 2008; 10: 45-51.
 9. Xiao M, Yang S, Chen J, Ning X, Guo L. Overexpression of MMSET in endometrial cancer: a clinicopathologic study. *J Surg Oncol.* 2013; 107: 428-32.
 10. Hudlebusch HR, Skotte J, Santoni-Rugiu E, Zimling ZG, Lees MJ. MMSET is highly expressed and associated with aggressiveness in neuroblastoma. *Cancer Res.* 2011; 71: 4226-35.
 11. Yang S, Zhang Y, Meng F, Liu Y, Xia B. Overexpression of multiple myeloma SET domain (MMSET) is associated with advanced tumor aggressiveness and poor prognosis in serous ovarian carcinoma. *Biomarkers.* 2013; 18: 257-63.
 12. Okabe H, Satoh S, Kato T, Kitahara O, Yanagawa R. Genome-wide analysis of gene expression in human hepatocellular carcinomas using cDNA microarray: identification of genes involved in viral carcinogenesis and tumor progression. *Cancer Res.* 2001; 61: 2129-37.
 13. Kassambara A, Klein B, Moreaux J. MMSET is overexpressed in cancers: link with tumor aggressiveness. *Biochem Biophys Res Commun.* 2009; 379: 840-5.
 14. Zhou P, Wu LL, Wu KM, Jiang W, Li JD. Overexpression of MMSET is correlation with poor prognosis in hepatocellular carcinoma. *Pathol Oncol Res.* 2013; 19: 303-9.
 15. Yang P, Guo L, Duan ZJ, Tepper CG, Xue L. Histone methyltransferase NSD2/MMSET mediates constitutive NF-kappaB signaling for cancer cell proliferation, survival, and tumor growth via a feed-forward loop. *Mol Cell Biol.* 2012; 32: 3121-31.
 16. Martinez-Garcia E, Popovic R, Min DJ, Sweet SM, Thomas PM. The MMSET histone methyl transferase switches global histone methylation and alters gene expression in t(4;14) multiple myeloma cells. *Blood.* 2011; 117: 211-20.
 17. Kuo AJ, Cheung P, Chen K, Zee BM, Kioi M. NSD2 links dimethylation of histone H3 at lysine 36 to oncogenic programming. *Mol Cell.* 2011; 44: 609-20.
 18. Jaffe JD, Wang Y, Chan HM, Zhang J, Huether R. Global chromatin profiling reveals NSD2 mutations in pediatric acute lymphoblastic leukemia. *Nat Genet.* 2013; 45: 1386-91.
 19. Asangani IA, Ateeq B, Cao Q, Dodson L, Pandhi M. Characterization of the EZH2-MMSET histone methyltransferase regulatory axis in cancer. *Mol Cell.* 2013; 49: 80-93.
 20. Nelson CE, Hersh BM, Carroll SB. The regulatory content of intergenic DNA shapes genome architecture. *Genome Biol.* 2004; 5: R25.
 21. Garcia-Carpizo V, Sarmentero J, Han B, Grana O, Ruiz-Llorente S. NSD2 contributes to oncogenic RAS-driven transcription in lung cancer cells through long-range epigenetic activation. *Sci Rep.* 2016; 6: 32952.